Article:

Hu, H., Papastergiou, P., Angelakopoulos, H. et al. (2 more authors) (2018) Mechanical properties of SFRC using blended manufactured and recycled tyre steel fibres. Construction and Building Materials, 163. pp. 376-389. ISSN 0950-0618

https://doi.org/10.1016/j.conbuildmat.2017.12.116

MECHANICAL PROPERTIES OF SFRC USING BLENDED MANUFACTURED AND RECYCLED TYRE STEEL FIBRES

Hang Hu[a*], Panos Papastergiou[a], Harris Angelakopoulos[b], Maurizio Guadagnini[a], Kypros Pilakoutas[a]

[a] Dept. of Civil and Structural Engineering, The University of Sheffield, Sir Frederick Mappin Building, Mappin Street, Sheffield, S1 3JD, UK. Tel: +44 (0) 114 222 5729, Fax: +44 (0) 114 2225700

[*] Corresponding author's email: hhu6@sheffield.ac.uk;

[b] Twincon Ltd, 40 Leavygreave road, Sheffield, South Yorkshire, S3 7RD, UK

ABSTRACT

This paper investigates the mechanical properties of 10 steel fibre reinforced concrete (SFRC) mixes at fibre dosages of 30, 35 and 45 kg/m^3. Manufactured Steel Fibres (MSF) are used on their own, or blended with sorted steel fibres recycled from end-of-life tyres (RTSF). To characterise the flexural behaviour of the mixes, two flexural test methods, BS EN 14651:2005 3-point notched prism tests and ASTM C1550-05 centrally loaded round panel tests are employed. A strong correlation is found in the flexural behaviour of the SFRC prism and round panel specimens, with corresponding conversion equations proposed. The mechanical properties of hybrid mixes using RTSF vary depending on dosages, but are comparable with those of MSF-only mixes at the same fibre dosage. A positive synergetic effect is derived from hybrid mixes containing 10 kg/m^3 of RTSF.

Keywords: SFRC; Recycled tyre steel fibres (RTSF); Hybrid steel fibres; Flexural performance; 3-point notched prism tests; Centrally loaded round panel tests; Synergetic effect.

1 INTRODUCTION

Annually about 1.5 billion tyres are produced and around 1 billion tyres (17 million tonnes) [1] reach their end of life worldwide[2]. To minimise the environmental impact of end-of-life tyres and generate value, the tyre recycling industry has developed various processes to extract the main tyre constituents (rubber, steel and polymer) [3]. The most commonly used and financially viable tyre recycling techniques adopt a combination of mechanical shredding and granulation, which produces steel fibres of irregular shapes, lengths and diameters. However, these fibres are often heavily contaminated with rubber (up to 20% by mass) and are prone to agglomeration due to significant geometrical irregularities and excessive aspect ratios. Further processing is thus required to: (1) minimise rubber contamination to less than 0.5% by mass, (2) limit the fibre length and diameter distribution to those that are effective in concrete (3) and avoid agglomeration before and during concrete mixing. Only after the tyre wire has been cleaned, sorted and classified, the product (“Recycled Tyre Steel Fibres” (RTSF)) can satisfy the Quality Assessment requirements for construction materials and thus can be used in concrete as structural reinforcement. Since 1999, numerous studies have been conducted at The University of Sheffield to investigate the mechanical properties of RTSF [4–10] and their potential in structural applications [11–15], and a patent application was filed in 2001 [16]. A spin-out company now produces classified RTSF. Comparative LCA studies [17,18] have shown that the RTSF production consumes only up to 5% of the energy required for the production of typical Manufactured Steel Fibres (MSF), highlighting the significant environmental benefits of RTSF.

MSF are commonly used as reinforcement in concrete applications such as industrial flooring [3,19,20] and tunnel linings [21]. Previous research [20,22–29] showed that the incorporation of steel fibres can significantly enhance the post-cracking residual strength, ductility and flexural toughness of a cementitious matrix, whilst their influence on compressive strength and modulus of elasticity is relatively small, unless a high fibre dosage is used [30]. However, in the majority of SFRC applications [26], only single-type fibre (i.e. MSF) reinforced concrete is used. The use of single-type fibres can be effective in arresting or bridging cracks of specified widths, but the fracture process of concrete matrix is more multi-scale and gradual [26]. The use of blended fibres with different aspect ratios (length/diameter) and physical properties (“fibre hybridisation [23]” in concrete), may provide better crack control over a broader range of crack widths. Several studies [23,25–27,29,31–35] on hybrid FRC (or mortar) have demonstrated that fibre hybridisation can lead to a better performance than that of single-type fibres. Khaleel et al. [36] reported that hybrid SFRC using 1% (by mass) of cleaned and sorted RTSF blended with 1% of undulated MSF exhibited higher flexural strength and toughness, compared to SFRC mixes containing 2% of undulated MSF. Nevertheless, this positive synergetic effect has not always been observed in previous studies using recycled tyre wire due to fibre agglomeration or unsuitable fibre combinations [33,37], in particular when unclassified and unsorted fibres were used. Since RTSF have a wide fibre length distribution and a higher nominal tensile strength than typical MSF, the mechanical properties of hybrid SFRC containing both MSF and classified RTSF, at different dosages, needs to be investigated. The results presented in this study are part of the FP7 EU-funded project "Anagennisi" [38] which aimed to develop uses for all tyre components in concrete.

Uniaxial tension tests for SFRC are difficult to conduct and interpret [11,12,30,39] and as a consequence flexural tests have become the preferred method to characterise the post-cracking residual flexural tensile strength and flexural toughness of SFRC. Nonetheless, various testing methodologies are available in different design codes of practice (Europe: [30,40–45], US: [46–48], Japan: [49]) and several researchers have developed their own test methods [50–52], including 3 or 4-point prism and single-point loaded, square slab and round panel tests. Compared with 4-point un-notched prism and square slab tests, BS EN 14651:2005 3-point (or even 4-point) notched prism [41] and ASTM C1550-05 round panel tests [48] have the advantage of generating consistent and predictable modes of failure [52], leading to a better comparison between different materials tested. Hence, these two tests are more universally adopted than others.

FRC test results are characterised by high variability due to non-uniformity in fibre distribution. Furthermore, test results from prisms are often associated with a larger scatter when compared to those from round panels, mainly due to significant differences in the fracture zone (roughly 187 cm^2 for prisms whilst 900 cm^2 for round panels). As a consequence of this, a minimum number of 12 tests for prisms [53] and 3 tests [48] for round panels are required per mix. It should be noted that prisms come with the extra requirement of saw cutting for notching, but the actual test is simpler and only requires a small-capacity testing machine.

Owing to the extensive experimental workload required, only one of the two testing methods is adopted in most research studies [14,20,51,52,54–58], which makes comparisons difficult. For the design of SFRC structures, the post-cracking residual flexural tensile strength f_R of SFRC prisms is commonly adopted in RILEM TC 162-TDF [40], CEB FIP Model Code 2010 [30], and Concrete Society TR 34 [45]. This underscores the need to determine this quantity accurately and to correlate the results from the standard 3-point notched prism tests and the round panel tests used in the American practice. One problem associated with such a correlation is that different fracture parameters are adopted in these two tests. f_R values at specified crack mouth openings (CMODs) are used for prism tests, while energy absorption capacity

(E values) up to selected deflections are adopted for round panel tests. Furthermore, flexural tensile strength $f_{ctm,fl}$ of the prisms can be calculated from the ultimate load of the load-deflection curves, but its counterpart from round panels is not included in ASTM C-1550. Bernard [20] proposed a calculation for the flexural strength based on the yield line theory for ASTM round panels, but the size of the loading plate (area of load) was not considered. Limited studies [20,51,52,59,60] have investigated the correlation between SFRC prisms with different geometric characteristics and round panel tests with regard to fracture parameters, but only MSF or some synthetic fibres (e.g. polypropylene fibres) were examined. The correlations between 3-point notched prism and round panel tests for steel fibre hybrids are rare and inconclusive, especially when RTSF is incorporated.

To address several of the above issues, the flexural performance of 10 SFRC mixes, using MSF on their own or blended together, is examined in this study employing both prism and round panels. This paper is structured as follows, section 2 introduces the experimental details of this study, including the geometrical and mechanical characterisation of both MSF and RTSF, the experimental campaign and concrete mix design. Section 3 presents the experimental results of SFRC under uniaxial compression and flexure (using two types of tests). Thereafter, correlations between the two flexural tests and the synergetic effect in hybrid mixes are discussed. Section 4 presents the design considerations of using hybrid SFRC reinforced with RTSF in structural applications and section 5 summarises the key research findings.

2 EXPERIMENTAL DETAILS

2.1 Fibre characterisation

RTSF (Figure 1 (a)) and two types of manufactured undulated (crimped) steel fibres, MSF1 (Figure1 (b)) and MSF 2 (Figure 1 (c)) were used in the study. Previous studies conducted by Neocleous et al. [13] suggests that RTSF with an aspect ratio greater than 200, can induce fibre balling even at low fibre dosages. A photography system was developed to determine the length and aspect ratio distribution of RTSF [15]. The system captures images of fibres passing in front of a screen with a high-speed camera and analyses the geometry of each fibre. The length distribution of a representative sample of approximately 60,000 fibres was found to be 68% (by mass) between 15-40 mm (Figure 2 (a)) with a mean length of 23 mm. Figure 2 (b) shows a histogram of the RTSF aspect ratio distribution, where a mean value of around 110 has been obtained. MSF1 had greater length, diameter and tensile strength than MSF2. Table 1 summarises the geometrical and mechanical characteristics of the three fibre types.

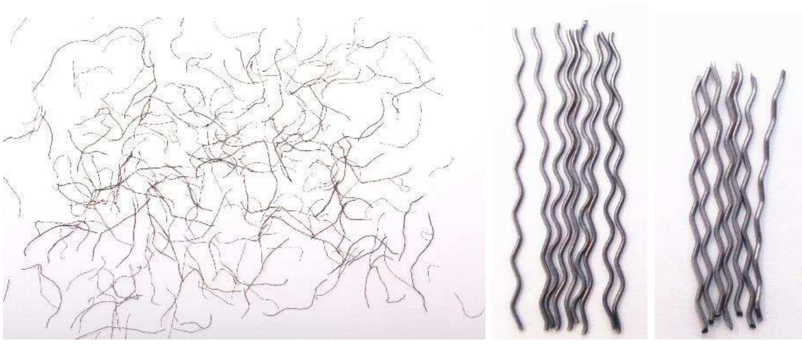

(a) (b) (c)

Figure 1: (a) RTSF, (b) MSF1 and (c) MSF2

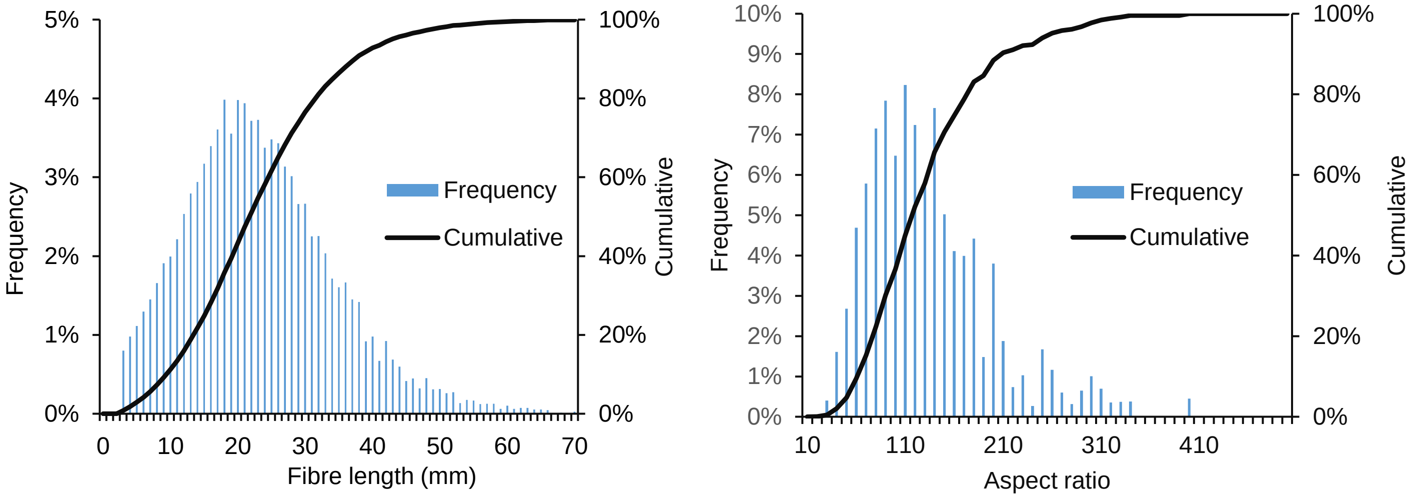

(a) (b)

Figure 2: RTSF histograms: (a) fibre length distribution; (b) aspect ratio distribution

Table 1: Geometrical and mechanical specifications of RTSF, MSF1 and MSF2

Fibre type	Length (mm)	Diameter (mm)	Aspect ratio	Tensile strength (MPa)	Elastic modulus (GPa)
a - RTSF	23*	0.22*	100*	2570*	200
b - MSF1	60 ± 2	1.0 ± 0.04	60.0	1450	200
c - MSF2	55 ± 2	0.8 ± 0.04	68.8	1050	200

* The nominal values for RTSF

2.2 SFRC mixes tested and mix design

Steel fibre dosages ranging between 30-45 kg/m^3 are commonly used in structural applications such as slabs-on-grade and suspended slabs on piles, to resist flexural and punching shear failure modes. Hence, two fibre dosages, were mainly investigated in this study: 30 kg/m^3 (volume fraction $V_f = 0.38\%$) and 45 kg/m^3 ($V_f = 0.57\%$). An additional mix of 35 kg/m^3 ($V_f = 0.45\%$) (mix F) was also tested to evaluate the performance of the higher strength MSF1 fibre at a lower dosage than the typical dosage of 45 kg/m^3 used in suspended slabs. A RTSF-only mix at 45 kg/m^3 was also tried but discarded due to balling issues, indicating the critical fibre dosage of RTSF using a conventional mixer is about 30 kg/m^3. A higher dosage of RTSF up to 36 kg/m^3 was reported by Centonze et al. [61] when a planetary mixer was employed. Table 2 shows details of the mixes including fibre type examined and their dosage.

To characterise the flexural and compressive properties of SFRC, 12 (or 6) prisms, 3 round panels and 6 cubes were cast per mix. Only 6 prisms were cast for mixes C, D, E, I and J to have a more comprehensive parametric investigation with less experimental workload. Due to the large volume of concrete required, the SFRC mixes were cast in 5 separate batches of ready-mixed concrete. For each batch, 6 plain concrete prisms and 6 cubes were also cast and then tested as control specimens.

Table 2: Experimental campaign

Total fibre dosage (kg/m^3)	Mix	Batch no.	Plast. (L/m^3)	Additional Water (L/m^3)	Slump (mm) before/after	MSF1 dosage (kg/m^3)	MSF2 dosage (kg/m^3)	RTSF dosage (kg/m^3)	Avg. f_{cu} (MPa) SFRC/Plain	Stdev. (MPa) SFRC/Plain
30	A	3	1.8	6.6	20/70	-	30	-	43.9/42.0	1.8/0.9
	B	4	1.5	3.3	60/120	-	20	10	42.6/46.1	2.2/2.0
	C	1	1.5	0	100/100	-	15	15	44.3/47.5	1.9/1.1
	D	1	1.5	0	100/100	-	10	20	44.6/47.5	1.9/1.1
	E	5	1.5	3.3	50/150	-	-	30	41.8/37.6	1.9/3.7
35	F	3	1.8	6.6	20/70	35	-	-	42.9/42.0	1.9/0.9
45	G	3	1.8	6.6	20/70	45	-	-	41.9/42.0	1.0/0.9
	H	4	1.5	3.3	60/120	35	-	10	42.8/46.1	0.2/2.0
	I	1	1.5	0	100/100	22.5	-	22.5	50.3/47.5	2.4/1.1
	J	2	1.5	3.3	30/80	10	-	35	44.5/39.9	0.7/1.0

The fibres were added manually during mixing, and vibration was applied after the moulds were filled with concrete. The specimens were cured in the moulds for 48 hours. After demoulding, all specimens were covered with wetted hessian fabric and plastic sheet was placed on top to retain moisture for the duration of curing, at a temperature of 22 ± 3 ℃. After 28 days of curing, all hessian and plastic sheets were removed and specimens were left to dry. All specimens were tested at the age of 35-60 days.

The workability of concrete can be affected adversely by fibre inclusion [62,63]. Though the slump test is not the best indicator of workability for SFRC materials (ACI 544.2R-89 [64]), it is still useful as a qualitative measure to maintain a consistent workability of concrete from batch to batch and it is still extensively used by the flooring industry. The common procedure adopted by the flooring industry for adding fibres in concrete was followed: The initial slump of the delivered ready mix concrete was taken which ranged from 20 to 100 mm (see Table 2) and additional water was added to the concrete mix if the measured slump was lower than 100 mm. After the addition of the water, the slump was checked again to reach at least 70 mm. Superplasticiser was then added which caused a collapse slump (beyond 260 mm). After the addition of fibres, the slump reduced to roughly the same levels as after the addition of the water (70-150 mm). No major fibre agglomeration has been observed during all 5 concrete castings; the target concrete compressive strength, f_{cu}, was 40 MPa. The concrete mix design was 150 kg/m^3 of cement, 150 kg/m^3 of GGBS, 1097 kg/m^3 of coarse aggregates (4-20 mm), 804 kg/m^3 of coarse gravel aggregates (0-4 mm). The initial water cement ratio (w/c) was 0.55.

2.3 Compressive cube tests: specimens preparation and testing procedure

The concrete cubes (150 mm) were tested under uniaxial compressive loading according to BS EN 12390-3: 2009 [65]. The dimensions of each cube were recorded before testing.

2.4 Flexural tests on prisms: specimens preparation and testing procedure

According to BS EN 14651:2005 [41], a notch (5 mm thick and 25 mm deep) was sawn at mid-span of each prism (150 mm x 150 mm x 550 mm) a day before testing. All prisms were tested under 3-point bending (Figure 3), using a 300 kN universal electromechanical testing machine. Two central deflections were recorded on either side of the specimens using two Linear Variable Differential Transformers (LVDTs), placed on an aluminium yoke. The Crack Mouth Opening Displacement (CMOD) was also measured at mid span with a 12.5 mm clip gauge (mounted under the notch of the prism). The loading point was free to rotate both in-plane and out-of-plane and the appropriate horizontal degrees of freedom were enabled at the supports. The tests were CMOD-controlled at a constant rate of 0.05 mm/min for CMOD from 0 to 0.1 mm and 0.2 mm/min for CMOD from 0.1mm until 4 mm. The dimensions of each specimen, including the distance between the tip of the notch to the top of each specimen were recorded before testing. All cracks initiated from the notch tip and then propagated to the top of the prism.

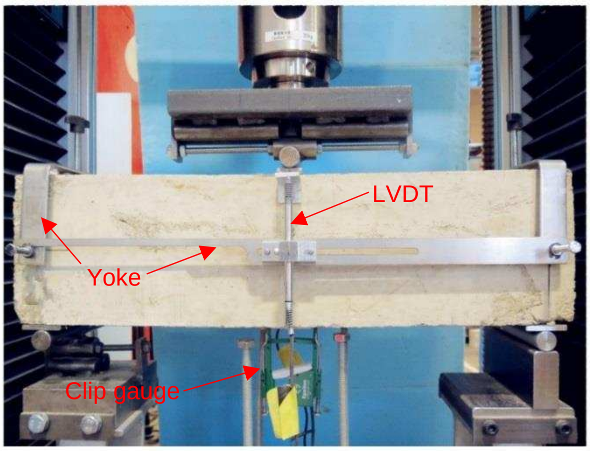

Figure 3: Flexural prism testing setup

2.5 Flexural tests on round panels: specimens preparation and testing procedure

The SFRC round panels were tested using a 250 kN hydraulic actuator, following the testing arrangement and procedure of ASTM C1550-05 [48]. Each round panel was centrally loaded and supported on three symmetrically (120°) arranged pivots on a pitch circle diameter of 750 mm (Figure 4). The test was under displacement control at a constant central deflection rate of 4 mm/min up to a maximum central deflection of 45 mm. Cracks initiated from the bottom central point of the panel and gradually propagated to the edges between the supports, forming three radial cracks at angles of 120°. Due to the random distribution of aggregates and fibres, the principal cracks do not propagate in a straight line (Figure 5). Furthermore, a large number of secondary cracks developed from the macrocracks.

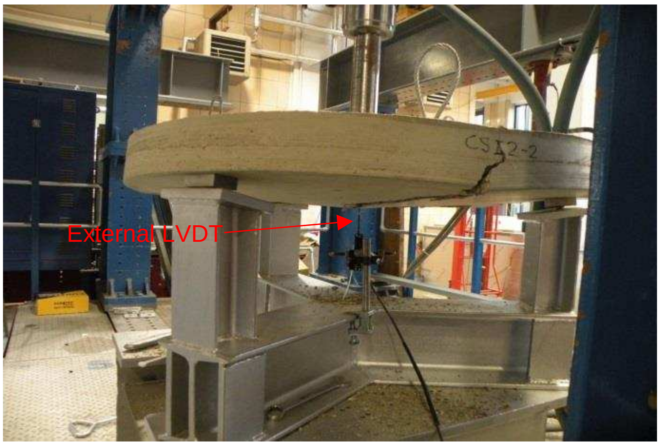

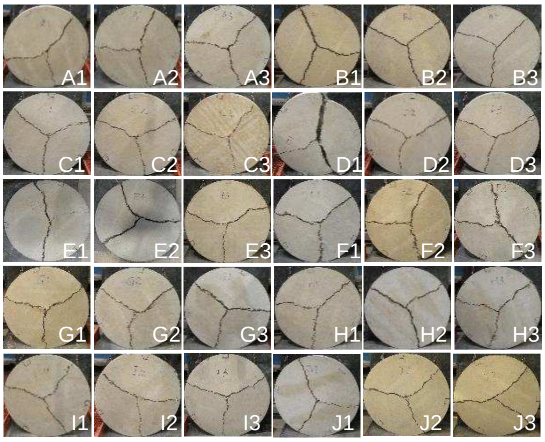

Figure 4: Flexural round panel test setup

Figure 5: Flexural round panel testing setup

3 EXPERIMENTAL STUDIES AND RESULTS

3.1 Compressive tests

The SFRC cube compressive strength f_{cu} ranged from 41.8 to 50.3 MPa, whilst the plain concrete compressive strength ranged from 37.6 to 47.5 MPa (see Table 2). The variability found is considered typical for ready mixed concrete. Compared to plain concrete, the compressive strength marginally increased up to approximately 5% due to the addition of MSF only, while an increase of around 10% was observed for mix E [RTSF (30)]. For hybrid mixes there was a small loss of strength (roughly 7%) at total fibre dosage of 30 kg/m^3, while at 45 kg/m^3, the strength change ranged from -7% to 11 %. Overall, the compressive strength of the hybrids was slightly better when using a higher dosage of RTSF.

In literature, the influence of steel fibres on the compressive strength of concrete is still inconclusive. For MSF, up to around 20% increase of compressive strength is reported by [29,62,66] when up to 78kg/m^3 of fibres was added, whilst a marginal effect or even a reduction up to 10% of compressive strength can be found in [67,68]. Very few studies investigated the effect of RTSF on the compressive strength of concrete. Up to 20% of enhancement was reported in [9,61,63] when adding no more than 48 kg/m^3 of RTSF, whilst a marginal effect was also reported in [33,35]. The variability in compressive strength can be explained by the fact that air trapped around fibres can decrease the strength [3], whilst fibres can arrest lateral microcracks and delay their coalescence in macrocracks, leading to marginal increases in strength. A significant reduction up to 20% was reported in [69] for concrete with unclassified and unsorted steel beads from waste tyres. This reduction in strength may be due to rubber (in free form or attached to the steel), and the highly variable geometrical characteristics of the beads that are prone to agglomeration. This highlights the importance of using clean and classified RTSF to limit variability.

3.2 Flexural prism tests

3.2.1 Relationship between measured deflection and CMOD values

The mid-span deflection of a prism, was taken as the mean of the deflection values measured from the 2 vertical LVDTs. It is noted that both vertical displacement measurements were in good agreement (see Figure 6) indicating little torsional effects, as also found by Soutsos et al. [66].

A linear relation between CMOD and average deflection is proposed by BS EN 14651:2005 [41], as given below,

$$Averaged\ \ deflection\ (mm) = k * CMOD\ (mm) + 0.04\ mm,\ k = 0.85 \quad (1)$$

This has been also confirmed by this study, where a very strong correlation was found between CMOD and averaged deflection values for all SFRC prisms tested. k ranged from 0.77 to 0.82, with coefficients of determination $R^2 > 0.99$.

Slightly higher values of k than those proposed by BS EN 14651 was reported in [51] when adding 45 kg/m^3 of hooked-end MSF with an aspect ratio of 66.7 in concrete. A linear relation between CMOD and average deflection employing 4-point notched SFRC prism tests was reported in [37], when both MSF and unsorted RTSF were used. The linear relationship between CMOD and deflection values allows for the possibility of measuring just one of them in the prism test.

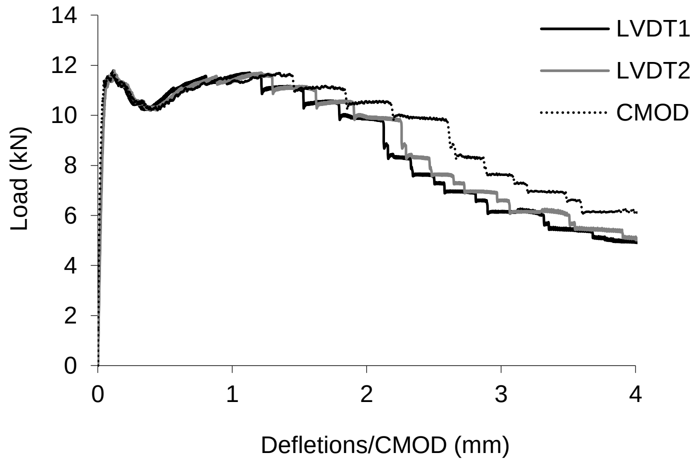

Figure 6: Typical deflection values obtained from two LVDTs and CMOD

3.2.2 Load-deflection curves

Since load-CMOD curves showed very similar behaviour to load-deflection curves, only the load-deflection curves are presented and discussed in this section. Figures 7 and 8 show the load-deflection curves for SFRC mixes at 30 kg/m^3, and 45 kg/m^3 (and also 35 kg/m^3), respectively. Load-deflection curves for single-fibre-type reinforced concrete and plain concrete prisms are shown in solid lines, while hybrid SFRC prisms are shown in dashed lines.

The solid red curves indicate the typical brittle behaviour of plain concrete, which highlights the weakness of concrete in tension. Generally, improved flexural performance can be obtained from concrete with higher total fibre dosage, from 30 kg/m^3 to 45 kg/m^3. The 35 and all 45 kg/m^3 mixes exhibited deflection hardening behaviour, which was only found from hybrid mix B [MSF2 (20) + RTSF (10)] at the total fibre dosage of 30 kg/m^3.

The best flexural performance was found from hybrid mixes B [MSF2 (20) + RTSF (10)] and H [MSF1 (35) + RTSF (10)] in the two groups of mixes, indicating that hybrid SFRC mixes containing 10 kg/m^3 of RTSF can show better flexural performance than MSF-only mixes at the same fibre dosage. Compared to other SFRC mixes, a sharper descending gradient occurs for mixes containing more than 22.5 kg/m^3 of RTSF (RTSF-only mix E and hybrid mixes I and J) starting at a deflection of approximately 1.5 mm. This may be due to the fact that shorter RTSF can debond or even pull out at large crack widths, leading to progressive damage. This also suggests that RTSF, due to their geometrical characteristics, are less effective at controlling macrocracks than MSF, as also reported by Graeff et al. [7] for fatigue tests and Zamanzadeh et al. [54].

CEB-FIP Mode Code 2010 [30] relates the constitutive laws of FRC at the SLS and ULS to the CMODs of 0.5 mm and 3.5 mm for the prism tests, respectively. This implies that the contribution of RTSF can be more beneficial at service conditions, but less helpful at large displacements or crack widths.

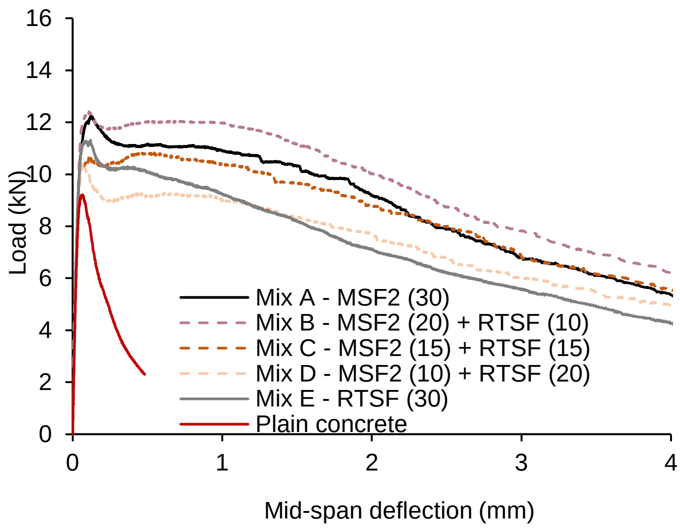

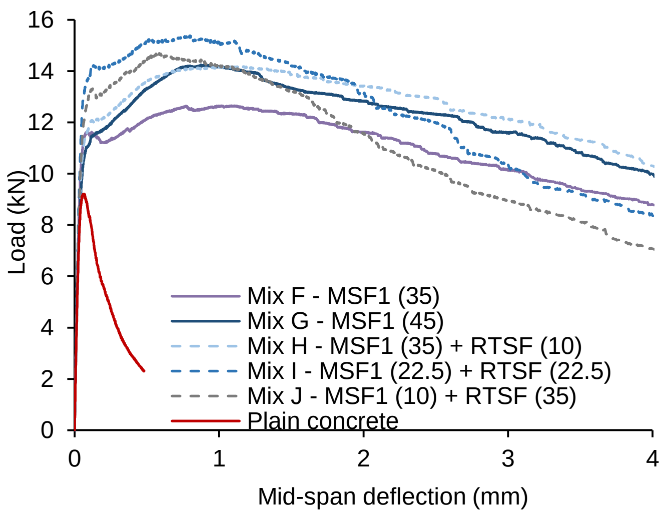

Figure 7: Load-deflection curves for SFRC mixes at 30 kg/m^3

Figure 8: Load-deflection curves for mixes at 35 and 45 kg/m^3

3.2.3 Flexural modulus of elasticity (E_{fm}), residual flexural tensile strength (f_R) and flexural tensile strength ($f_{ctm,fl-1}$)

Flexural modulus of elasticity (E_{fm})

The modulus of elasticity of concrete can be measured directly via compressive tests or indirectly via flexural tests. Elastic analysis was used to determine the flexural modulus (by matching results up to 40% of the ultimate flexural load) from flexural tests (Figure 9). Since the load spreading effect was found to be negligible [12], the dimensions of the loading and supporting rollers was not considered. Ignoring shear deformation in the prism, the linear equation relating the load-deflection stiffness to E_{fm} is given below,

$$E_{fm} = \frac{PL^3}{48I\delta} \tag{2}$$

Where $\frac{P}{\delta}$ (kN/mm) is the slope of the initial part of the load-deflection curve, L (mm) is the span of the prism, I (mm^4) is the second moment of area of the middle cross-section.

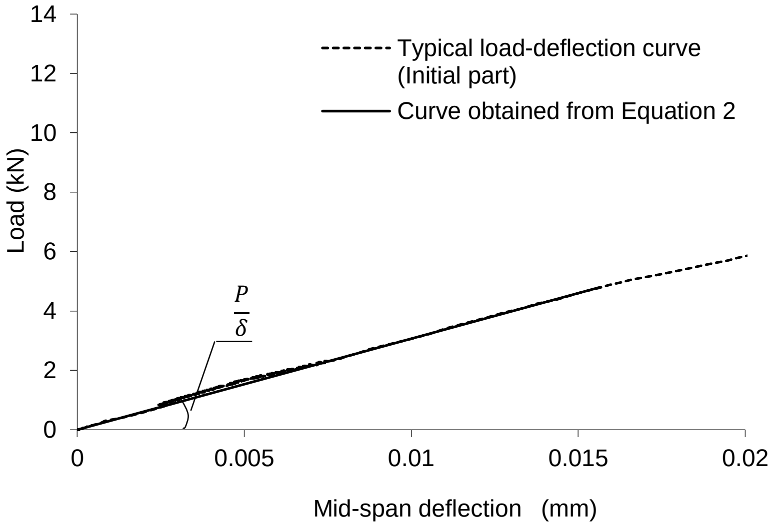

Figure 9: The determination of flexural modulus E_{fm}

Figure 10 shows the flexural modulus E_{fm} and related standard deviations of all SFRC mixes tested. The counterparts for plain concrete are shown in grey columns.

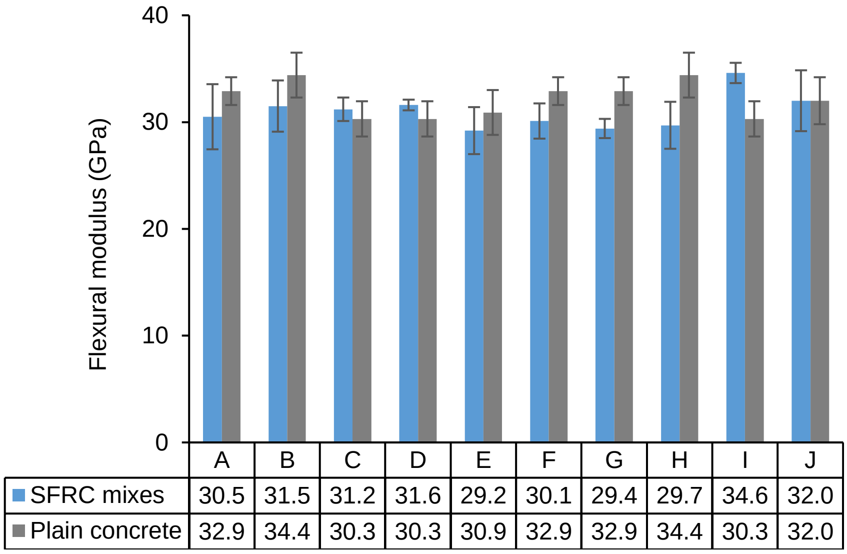

Figure 10: E_{fm} of SFRC and plain concrete prisms

All SFRC prisms showed similar E_{fm} to the plain concrete. A similar conclusion was also arrived by Jafarifar [14], when 60 kg/m^3 of RTSF (of slightly shorter lengths) was added to conventional concrete or roller compacted concrete. RTSF-reinforced mixes showed comparable moduli and standard deviations to MSF-only mixes. Air entrapped around the fibres could have a negative effect on the elastic modulus, while the steel fibres can contribute in a positive manner. Since both effects are small in low fibre dosages, no significant change in the elastic properties is expected.

Residual flexural tensile strength (f_R)

BS EN 14651:2005 [41] follows a methodology first adopted by RILEM TC 162-TDF [40], to characterise the residual flexural tensile behaviour of SFRC prisms, where flexural stresses (f_{R1}, f_{R2}, f_{R3} and f_{R4}) are calculated from the load-CMOD curves at 0.5, 1.5, 2.5 and 3.5 mm of CMOD, respectively. The calculation of f_R [41] for 3-point bending test is given below,

$$f_{Ri} = \frac{3F_{Ri}l}{2bh_{sp}^2} \tag{3}$$

Where F_{Ri} (N) is the applied load at CMODs of 0.5, 1.5, 2.5 and 3.5 mm ($i = 1,2,3,4$). $b = 150\ mm$ is the width of prism, $l = 500\ mm$ is the span length and h_{sp} is the distance between the tip of the notch to the top of the specimen.

Figure 11 shows the f_{Ri} values (in MPa) of all SFRC mixes. Coefficients of variation (COV) for those values are listed in brackets.

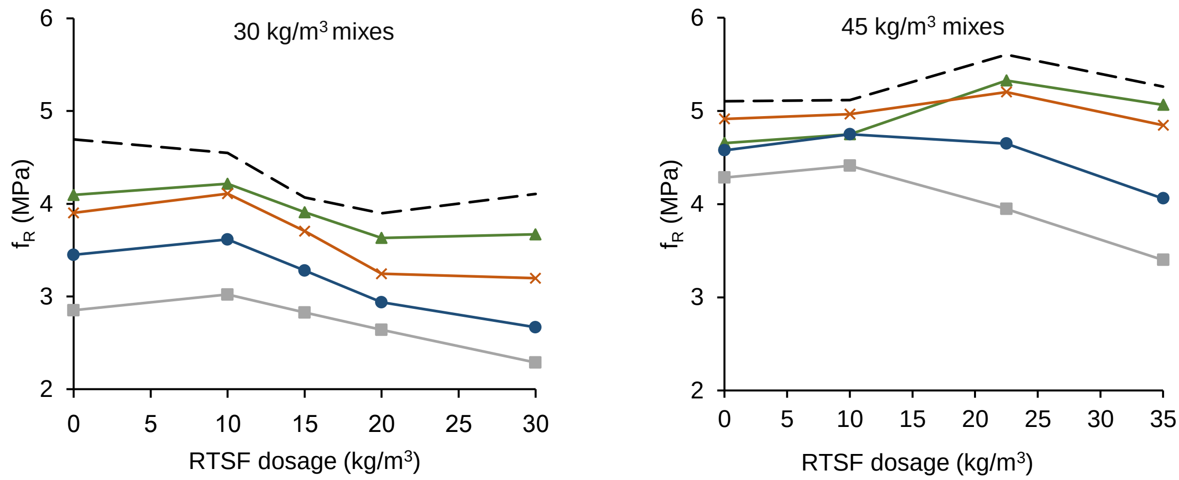

	A	B	C	D	E	F	G	H	I	J
$f_{ctm,fl\text{-}pc}$	3.1 (10%)	3.2 (9%)	3.0 (7%)	3.0 (7%)	3.0 (13%)	3.1 (10%)	3.1 (10%)	3.2 (9%)	3.0 (7%)	3.3 (9%)
$f_{ctm,fl\text{-}1}$	4.2 (17%)	4.0 (13%)	3.6 (6%)	3.4 (2%)	3.6 (7%)	4.3 (17%)	4.6 (18%)	4.6 (20%)	5.1 (14%)	4.8 (12%)
f_{R1}	3.6 (25%)	3.7 (16%)	3.4 (6%)	3.1 (6%)	3.2 (10%)	3.8 (19%)	4.2 (19%)	4.2 (21%)	4.8 (15%)	4.6 (14%)
f_{R2}	3.4 (27%)	3.6 (18%)	3.2 (7%)	2.7 (11%)	2.7 (12%)	4.0 (18%)	4.4 17%)	4.5 (21%)	4.7 (10%)	4.3 (10%)
f_{R3}	2.9 (32%)	3.1 (19%)	2.8 (8%)	2.4 (11%)	2.2 (16%)	3.7 (16%)	4.1 (14%)	4.2 (21%)	4.1 (11%)	3.6 (12%)
f_{R4}	2.4 (34%)	2.5 (25%)	2.3 (10%)	2.1 (19%)	1.8 (18%)	3.3 (17%)	3.8 (17%)	3.9 (24%)	3.4 (11%)	2.9 (13%)

Figure 11: $f_{ctm,fl-1}$ and f_R values of prisms (in MPa), and COV (in %)

Since plain concrete always fails in flexure before CMOD reaches 0.5 mm, f_R values and correspondant variability values for plain concrete mixes are not applicable. Figure 11 shows that f_{R4} values for 30 kg/m³ SFRC mixes are lower than the flexural tensile strength of the correspondent plain concrete, however, f_{R4} values for 35 kg/m³ and 45 kg/m³ mixes (apart from hybrid mix J containing 35 kg/m³ of RTSF) are higher, indicating that MSF are more effective at "bridging" macrocracks due to their longer length, larger diameter and deformed shape. The COV for the residual flexural tensile strengths for all mixes are within the range of 40%, which is in agreement with literature [51,54,70].

In this study, f_{R1} and f_{R2}, f_{R3} and f_{R4} are shown to correlate to each other very well (Figure 12). In literature, a strong correlation between f_{R1} and f_{R4} was also reported in [67] for two types of hooked-ends MSF and linear relations between f_{R1} and f_{R3}, f_{R1} and f_{R4} were found by Zamanzadeh et al. [54] for unclassified RTSF. However, a strong correlation between f_{R1} and f_{R3} or f_{R4} was not found in this study.

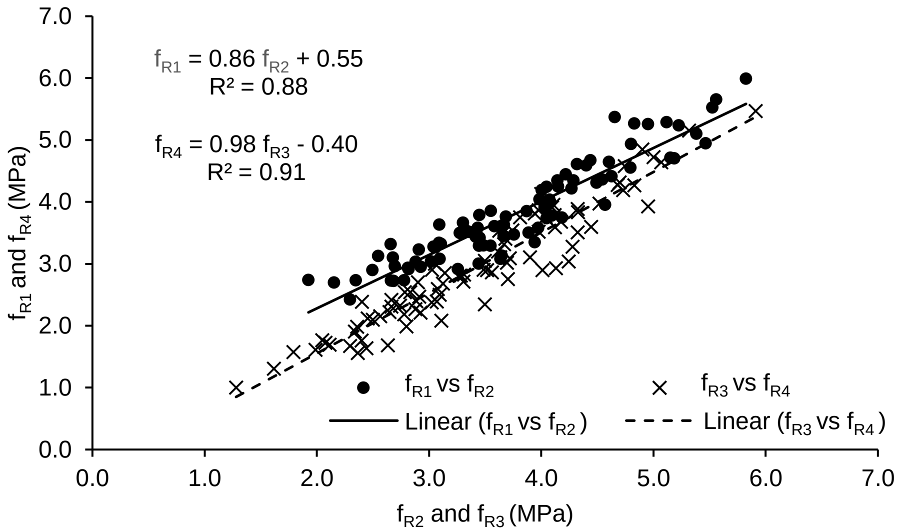

Figure 12: Correlation between f_{R1} and f_{R2}, f_{R3} and f_{R4} of all prisms

Flexural tensile strength ($f_{ctm,fl-1}$)

The concept of Limit of Proportionality (LOP), as a representation of the flexural tensile strength or initiation of flexural cracking, is adopted by BS EN 14651:2005 [41]. In an attempt to determine LOP values, it was found that the standard procedure is susceptible to initial recording errors and irregularities in the load-deflection curves. Similar observation was made by Neocleous et al. [6]. On the other hand, flexural tensile strength ($f_{ctm,fl}$), adopted in BS EN 12390-5 [44], is the stress obtained from the ultimate load of the load-deflection curves for 4-point prism bending tests. The use of $f_{ctm,fl}$ was found to be less subjective and more convenient to compare prism tests to panel tests, as discussed later. The calculation of $f_{ctm,fl}$ is given below, where F_u (N) is the ultimate load of the load-deflection curves.

$$f_{ctm,fl} = \frac{3F_u l}{2bh_{sp}^2} \quad (4)$$

In Figure 11, the subscript –pc for $f_{ctm,fl}$ values (in MPa) refers to plain concrete prisms, and -1 for SFRC prisms since 1 principal crack is always developed in the prism. Coefficients of variation (COV) for those values are listed in brackets, and the small COV for $f_{ctm,fl-pc}$ suggests that the set-up for prism tests is stable and reliable. It is noted that for SFRC mixes, the COV increases from $f_{ctm,fl-1}$, f_{R1} to f_{R4}. This can be explained by the fact that the post-cracking behaviour of SFRC depends increasingly more on fibre-matrix interaction, fibre distribution and orientation as cracks open, than the resistance provided by the matrix itself such as through aggregate interlock.

Compared to plain concrete of the same batch, $f_{ctm,fl-1}$ increased by approximately 15% to 40% and 45% to 70% at total fibre dosages of 30 kg/m^3, 45 (and 35) kg/m^3, respectively. This confirms the positive effect of steel fibres in arresting microcracks and delaying their coalescence to form macrocracks, and it is evident that higher total fibre dosages can lead to higher $f_{ctm,fl-1}$ values. At 30 kg/m^3, the use of blended fibres did not enhance the $f_{ctm,fl-1}$ values, whilst at 45 kg/m^3, hybrid mixes showed similar or higher flexural strength than mix G (45 kg/m^3 of MSF).

3.3 Flexural round panel tests

3.3.1 Deflection values measured by external and internal LVDTs

The flexural toughness is evaluated based on the energy absorption capacity at specific central deflections. A transducer was mounted centrally beneath the panel to measure central deflection. The deflection from this and the internal transducer of the actuator are compared in Figure 13. As expected, the initial part of the deflection behaviour is better represented by the external LVDT, due to the inclusion of extraneous deflections arising from deformation of the load frame and concrete crushing at the supports in the actuator displacement record. However, there is only a marginal difference in the post-cracking behaviour between the two sets of measurements.

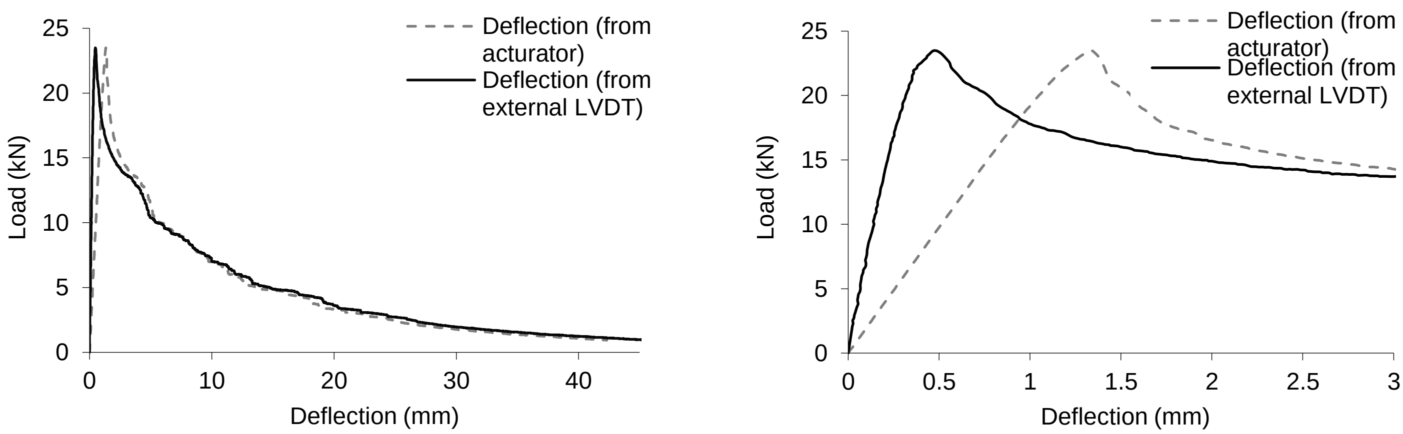

(a) (b)

Figure 13: Deflection measurements from actuator and external LVDTs (a) a typical load-deflection curve, (b) initial part of the curve

The diameter of each panel was measured prior to testing, using the average value of three measurements coincident with the support locations. After testing, the thicknesses of the panels were measured along the three principal cracks to estimate the average thickness; three measurements were taken along each crack and one in the centre (10 measurements in total). Both diameter and thickness measurements confirm that the panels tested were within the limits of the standard.

3.3.2 Load-deflection curves

Figures 14 and 15 show the load-deflection curves for SFRC round panels at the total fibre dosages of 30 kg/m³ and 45 kg/m³ (also 35 kg/m³), respectively. As opposed to the prism tests, only deflection softening behaviour is observed. The beneficial effect of increasing the total fibre dosage on the flexural behaviour of SFRC round panels can be seen, with mixes at 45 (and 35) kg/m³ demonstrating an enhanced peak load and flexural toughness, when compared to mixes at 30 kg/m³.

At 30 kg/m³, the best overall flexural performance was observed from hybrid mix B containing 10 kg/m³ of RTSF, whilst the lowest was found from RTSF-only mix E [RTSF (30)]. Blending RTSF with MSF results in a synergy that is able to combine the benefits of the individual fibre types at controlling cracks at different stages.

At 45 kg/m³, the best flexural behaviour was seen for hybrid mix I [MSF1 (35) + RTSF (10)]. Surprisingly, the increase of MSF1 dosage (comparing mix G to F) in concrete showed little change in the post-cracking behaviour of SFRC, which might be an indication that the 45 kg/m³ exceeds the optimum fibre content for this fibre type, as it can cause more balling and air trapped in the mix. In hybrid mixes, the replacement of MSF with more than 22.5 kg/m³ of RTSF (mixes I and J) showed the lowest post-cracking capacity at large cracks, confirming the limitations of RTSF in controlling large cracks due to a combination of fibre breakage and fibre pull-out.

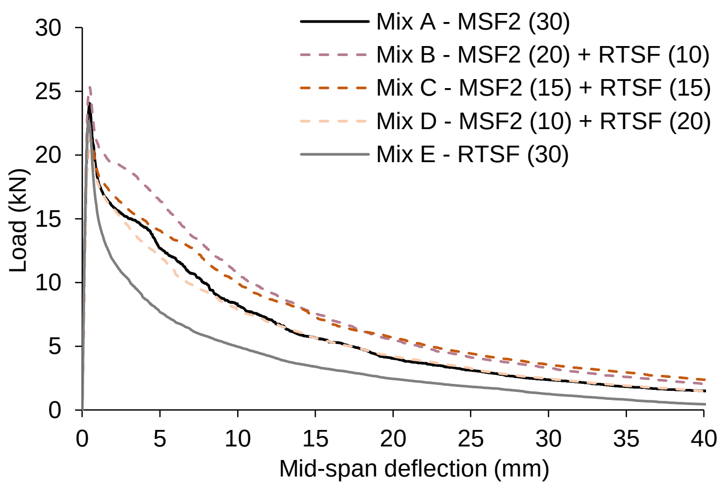

Figure 14: Load-deflection curves for SFRC mixes at 30 kg/m³

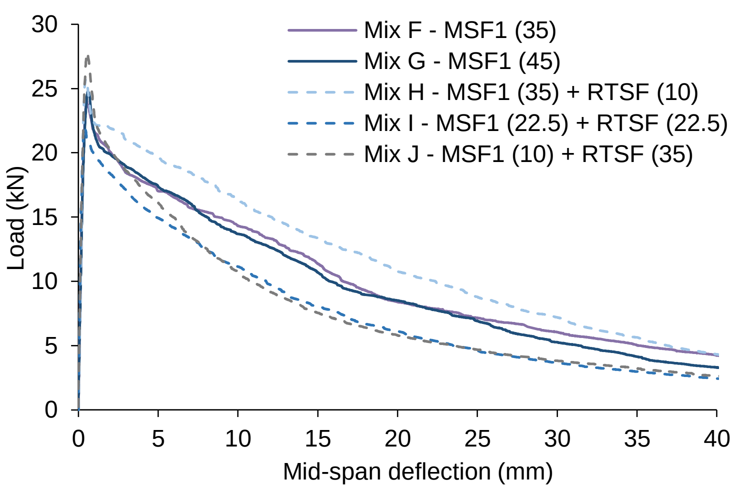

Figure 15: Load-deflection curves for SFRC mixes at 35 kg/m³ and 45 kg/m³

3.3.3 Energy absorption (E) and flexural tensile strength ($f_{ctm,fl-3}$)

Energy absorption capacity

To assess the flexural toughness of the round panels, the energy absorption capacity E' up to central deflections of 5, 10, 20 and 40 mm were obtained from the load-deflection curves according to ASTM C1550-05 [48]. As seen in Equation 5, a correction factor $\beta = 2 - (\delta - 0.5)/80$ is used to accommodate for the variability in thickness, since thickness has a more pronounced influence on the post-cracking behaviour of panels than diameter [20].

$$E = E' \left(\frac{d_0}{d}\right)^{\beta} \left(\frac{R_0}{R}\right) \tag{5}$$

Where δ (in mm) is the specified central deflection up to which the energy absorption capacity is calculated; $R_0 = 400\ mm$ and $d_0 = 75\ mm$ are the nominal round panel radius and thickness, respectively; R and d are the measured radius and thickness values.

Figure 16 shows the energy absorption capacity (E, in J) for all SFRC mixes and their corresponding COV (shown in brackets). In general, the 35 and all 45 kg/m^3 mixes showed higher energy absorption capacity than the 30 kg/m^3 mixes, confirming the positive effect of fibre dosage on flexural toughness.

Interestingly, the replacement of MSF with varying dosages of RTSF did not affect the variability of flexural toughness. The flexural tensile strength ($f_{ctm,fl-3}$, in MPa) and the corresponding COV are presented in Figure 16, as discussed later.

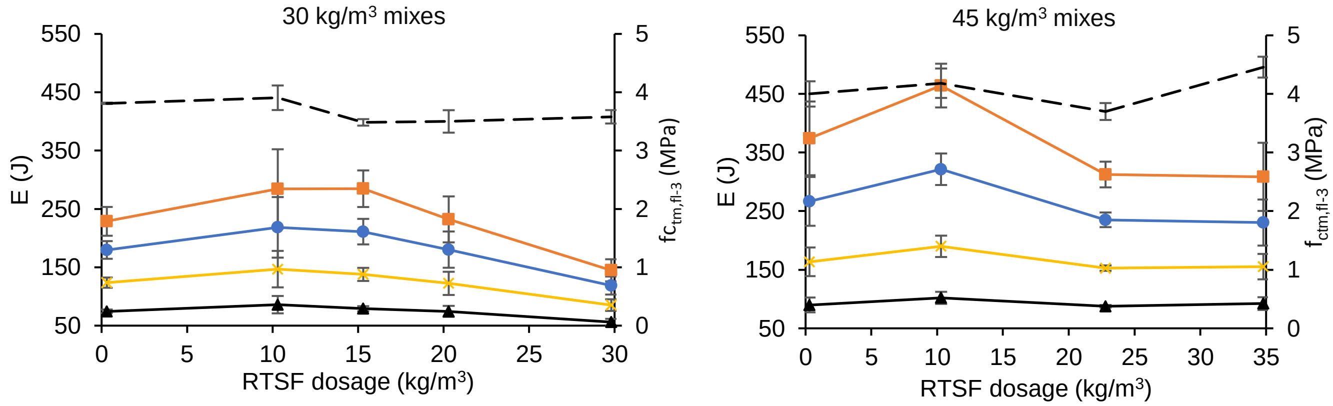

	A	B	C	D	E	F	G	H	I	J
— — $f_{ctm,fl-3}$	3.7 (0%)	3.8 (5%)	3.4 (2%)	3.5 (6%)	3.5 (3%)	3.6 (4%)	3.8 (5%)	4.1 (6%)	3.7 (4%)	4.3 (4%)

E_5	74 (4%)	86 (14%)	79 (5%)	75 (10%)	56 (8%)	86 (5%)	90 (12%)	102 (8%)	88 (2%)	92 (10%)
E_{10}	124 (6%)	147 (17%)	138 (7%)	122 (13%)	85 (10%)	157 (5%)	164 (12%)	190 (8%)	153 (3%)	155 (11%)
E_{20}	180 (7%)	218 (19%)	211 (9%)	180 (14%)	119 (11%)	262 (6%)	267 (13%)	321 (7%)	235 (4%)	230 (14%)
E_{40}	229 (9%)	285 (19%)	285 (9%)	232 (14%)	145 (11%)	379 (8%)	374 (14%)	464 (7%)	313 (6%)	309 (15%)

Figure 16: $f_{ctm,fl-3}$, E_5, E_{10}, E_{20} and E_{40} of SFRC round panels

Strong correlations are found between E_5 and E_{10}, E_{20} and E_{40} (Figure 17), possibly because the larger fracture zone activated can lead to a more consistent post-cracking behaviour than that of the notched prisms.

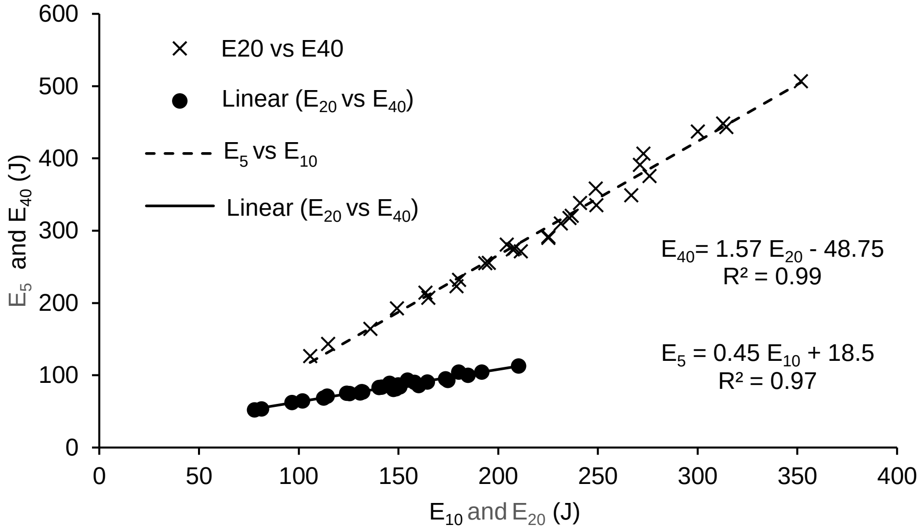

Figure 17: Correlations between E_5 and E_{10}, E_{20} and E_{40} of SFRC panels

Flexural tensile strength ($f_{ctm,fl-3}$)

As there is no direct correlation between the residual flexural tensile strength f_R and the energy absorption capacity E used by the two standards, a common parameter is needed to compare the results from the two tests.

The yield line theory developed by Johansen in 1972, is a practical method to provide an upper bound solution for the collapse load of a structure and can help obtain the flexural strength from panels [20]. Although the yield line method was originally developed for plastic materials, this approach has been found useful even for lightly reinforced SFRC. The Concrete Society TR 34 [45] adopts this method to determine the ultimate load capacity of FRC ground-supported slabs under different load combinations. Bernard [20] proposed an analytical relationship between the ultimate load and the moment of resistance per unit length at yield lines for the ASTM round panels. However, the loading actuator was taken as a point load, which underestimates the effect of the real load being applied through a circular plate, hence overestimates flexural strength. By considering the actual geometry of the loading plate (see Figure 18), the ultimate load can be determined as,

$$P_u = \frac{m[3\sqrt{3}(R-r)+2\pi r]}{R-r-c} \tag{6}$$

As for the prisms, the moment of resistance of the panel per unit length can be calculated by considering a linear elastic distribution of stress across the section,

$$m = \frac{1}{6} b d^2 \sigma_{max} \tag{7}$$

Hence, the flexural tensile strength $f_{ctm,fl-3}$ (since 3 principal cracks are always developed) of a SFRC round panel can be expressed as,

$$f_{ctm,fl-3} = \sigma_{max} = \frac{6P_u(R-c-r)}{bd^2[3\sqrt{3}(R-r)+2\pi r]} \tag{8}$$

Equation 8 shows that if the radius of the loading plate is ignored, the flexural tensile strength $f_{ctm,fl-3}$ can be overestimated by 18%.

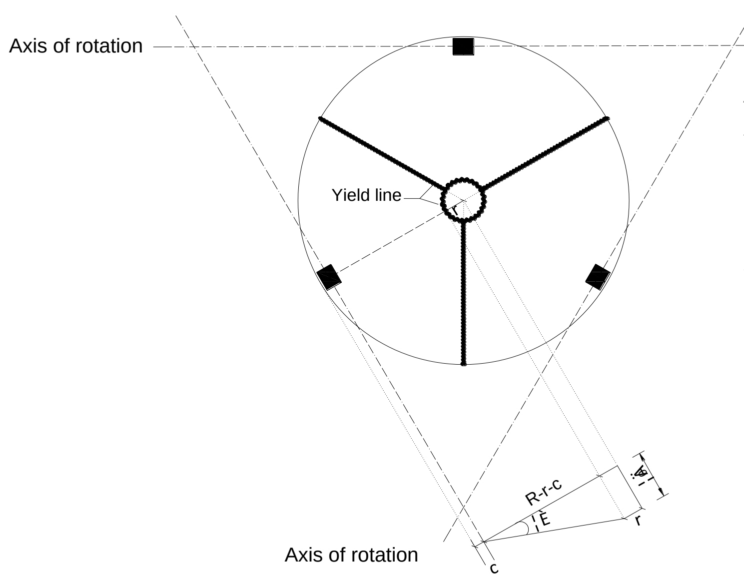

ASTM C1550-05:
$r = 0.05\ m$, the radius of the circular loading plate;
$c = 0.025\ m$, the distance between the edge of the panel and the central line of the support.
R (in m) is the radius (measured) of the round panel;
d (in m) is the thickness (measured) of the panel;
δ_0 is the unit vertical displacement induced by the concentrated load;
$b = 1\ m$ is the unit width of the panel; σ_{max} is the nominal maximum flexural stress of sections on yield lines.

Figure 18: Yield line analysis of an ASTM C1550-05 round panel

The circular yield line in the centre of the specimen (Figure 18), does not appear in the failure photos of the tested round panels at the bottom (Figure 5), as the potential failure (yield line) pattern is based on an assumption of perfectly plastic behaviour of a round panel. In fact, after loading, concentrated microcracking develops in a small region on the soffit of a lightly reinforced panel where the flexural capacity of SFRC has been exceeded. Furthermore, three main cracks starting from a point of maximum deflection will migrate to the edges between each pair of supports.

Figure 16 compares the values of $f_{ctm,fl-3}$ for all SFRC round panels. The largest $f_{ctm,fl-3}$ values are obtained from hybrid mixes B [MSF2 (20) + RTSF (10)] and J [MSF2 (10) + RTSF (35)] at 30 and 45 kg/m^3, respectively. COV for $f_{ctm,fl-3}$ for all mixes, are in the range of 0 - 6% (shown in brackets in Figure 16). For all mixes, the variability in the energy absorption capacity calculated at different deflection values increases with the increase in deflection and corresponding crack opening. This indicates the fibre-matrix interaction, fibre distribution and orientation became more predominant as cracks open.

3.4 Correlation in the behaviour of SFRC prisms and round panels

Since the fracture parameters (prisms: $f_{ctm,fl-1}$ and f_R values; panels: $f_{ctm,fl-3}$ and E values) represent the fracture properties of the same material, the flexural behaviour of the SFRC prisms and round panels is expected to be related.

The relation between $f_{ctm,fl-1}$ and $f_{ctm,fl-3}$ is shown in Figure 19. In general, the values from prisms $f_{ctm,fl-1}$ are up to 13% higher than those from round panels for 30 kg/m^3 mixes and 11 -18% (except for mix I) for 45 (and the 35) kg/m^3 mixes. This can be partly attributed to the different methodology used in each test. For example, in the prism tests the specimens are notched to force the crack to occur at a given location, hence the crack does not necessarily open at the section exhibiting the lowest material strength. In the round panels, however, the yield lines form naturally and follow the weakest sections. It is noted that the round panels have a much larger crack length (yield line equivalent) than the prisms and, hence, they are expected to show a lower COV as confirmed by the results in Figures 11 and 16.

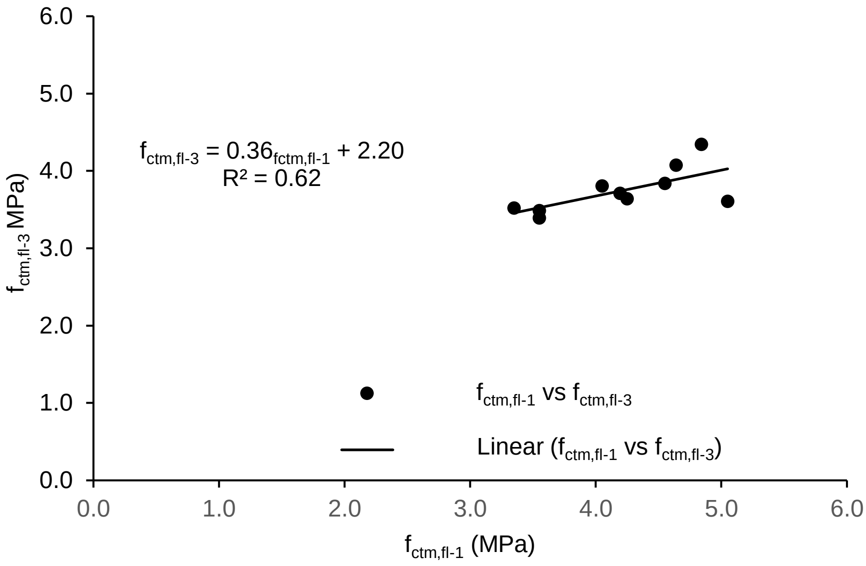

Figure 19: Correlations between $f_{ctm,fl-1}$ (prisms) and $f_{ctm,fl-3}$ (round panels)

Figure 20 shows the correlations between f_{R1} and E_5, f_{R4} and E_{40}. The weaker correlation between f_{R4} and E_{40} highlights the more variable behaviour of SFRC at large cracks, which can be influenced by the effectiveness of just a few fibres in the case of the prism tests. There is a reasonable correlation between f_{R1} and E_5, which indicates that the two tests, though dissimilar, they more or less provide the same information. These three mathematical correlations can help engineers to convert the fracture parameter, from one test to the other, at peak stress ($f_{ctm,fl-1}$ and $f_{ctm,fl-3}$), the SLS (f_{R1} and E_5) and ULS (f_{R4} and E_{40}). It is noted that the proposed equations are only valid for conversion between ASTM C1550-05 round panel tests and BS EN 14651:2005 prism tests. In order to better compare and exchange results obtained from different test methods, a broad database of specimens with varying geometry, loading scheme, concrete strength, fibre dosage and volume, is still required.

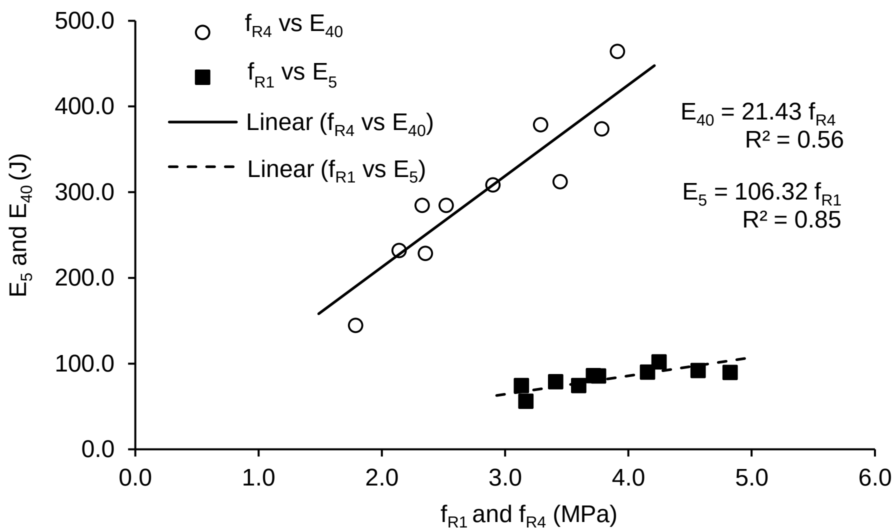

Figure 20: Correlations between f_{R1} (prisms) and E_5 (round panels), f_{R4} (prisms) and E_{40} (panels)

3.5 Synergetic effect in hybrid mixes

To quantify the synergetic effect in hybrid SFRC mixes, a synergy ratio S_i, which is a function of the normalised fracture parameters i of the hybrid mixes with those of the control mixes (MSF-only mixes A and G), is adopted:

$$S_i = (\frac{i_{hybrid}}{i_{MSF}} - 1) \times 100, \text{ in } \% \tag{9}$$

Where i represents the f_R values obtained from prism tests or E values derived from round panel tests. Figure 21 shows the S_{f_R} values (dashed lines) and the S_E values (solid lines) for all hybrid mixes.

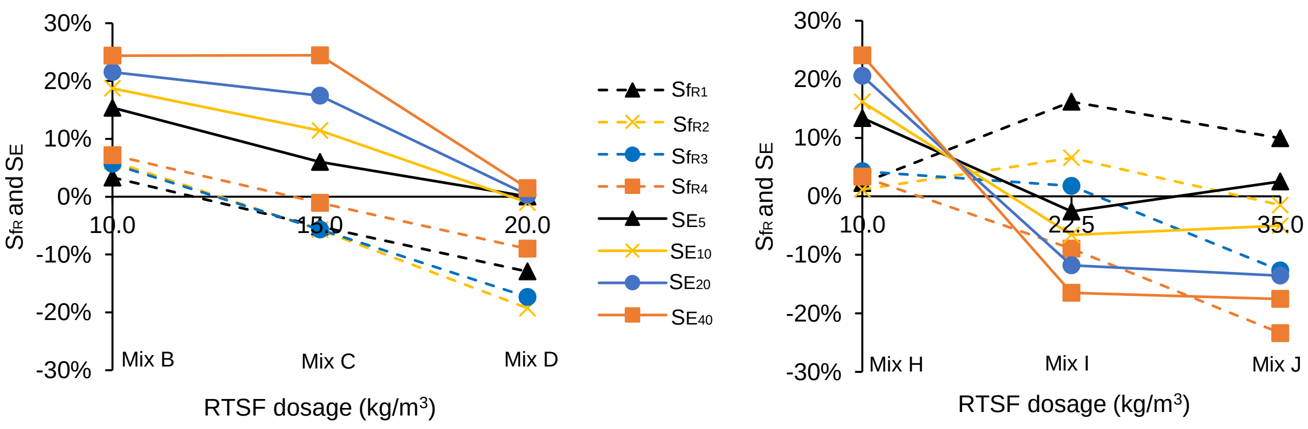

(a) (b)

Figure 21: Synergetic ratios S_i for hybrid mixes at (a) 30 kg/m³ (b) 45 kg/m³

3.5.1 Effect of test type

For the same mix, different and contradictory S_i values are observed for each type of test. For example, for hybrid mix C [MSF2 (10) + RTSF (20)], negative S_i values (-1% to -6%) are determined from the prism tests, whilst positive values (6 - 24%) are shown for the round panel tests. These differences can be explained by the: (1) nature of the parameter measured by f_R and E values - f_R is a local value of residual stress whist E quantifies all the energy under the curve; (2) magnitude of crack width - the crack widths in the round panels are much wider at the corresponding E values than at the f_R values of the prism tests; (3) length and nature of the fracture zone - in the prism tests the fracture zone is forced to occur at the notched section with a length of 150 mm, whilst in the panel tests the 3 fracture zones (each around 400 mm long) follow the weakest section in the region of maximum stress; (4) fibre orientation - as fibres are prone to orientating along boundaries, the fibres in the beams are more favourably oriented. Further research is thus needed to investigate the effect of fibre orientation and distribution (in particular for hybrid mixes) on the mechanical properties of multi-scale SFRC specimens.

3.5.2 Effect of fibre dosage

The overall trend (see Figure 21) in both tests shows that small amounts of RTSF (up to 10 kg/m^3) offer a significant synergetic effect, but as their quantity increases that effect diminishes and eventually reverses. As previously discussed, RTSF tend to be more effective than MSF in controlling microcracks, such that the hybrid mixes containing RTSF can perform better than MSF-only mixes at the initial microcracking stage. However, even at larger cracks the hybrid mixes containing a low RTSF dosage (i.e. 10 kg/m^3) also exhibit better performance than MSF-only mixes, despite RTSF being less effective in controlling macrocracks. A likely cause is that the better distribution of RTSF (due to higher fibre count as a result of their “fineness”) increases the strength of the concrete matrix (see $f_{ctm,fl-1}$ for mix E [RTSF (30)], Figure 11, compared to plain concrete), which can lead to an improved fibre-matrix interfacial bond performance and thus increased pull-out resistance of MSF. A positive fibre interlock effect may also be provided by the closely spaced RTSF, even though fibre interlock usually occurs at a high fibre percentage [11]. In the case of round panel tests, where new microcracks develop at different stages of loading, more RTSF are continuously engaged in controlling microcracking and dissipating energy. In contrast, for hybrid mixes containing a high dosage of RTSF (and less MSF), fewer MSF bridge macrocracks and this can lead to a significant degradation of the flexural performance at larger cracks, and potentially increase variability, as the behaviour of SFRC depends more strongly upon the location and orientation of fewer MSF.

4 DESIGN CONSIDERATIONS OF SFRC WITH RTSF UNDER FLEXURE

The positive synergetic effect between MSF and RTSF could lead to the reduction of slab thickness, less joints and less conventional reinforcement, as well as significant savings in construction time and labour cost. Hence, this synergy should be exploited during the design stage of concrete slab applications such as slabs-on-grade and suspended slabs.

4.1 Flexural tensile strength and uniaxial tensile strength of SFRC

For the SFRC mixes tested in this study, an increase of 13 - 70% in $f_{ctm,fl-1}$ was obtained when compared to the strength of plain concrete. As reported by ACI 544.1R-96 [19], the increase in the direct tensile strength of SFRC is much lower than that in the flexural tensile strength, since the stress-strain distribution in the tension zone of a specimen alters from elastic to nearly plastic after cracking. However, the uniaxial tensile stress-strain relationship proposed by RILEM TC 162-TDF [40] (Figure 22) suggests that the tensile strength (f_t) of SFRC is proportional to the LOP derived from the prism tests, whilst in Model code 2010 [30] an identical tensile strength as plain concrete is assumed when FRC shows softening or slight hardening behaviour. These two models can lead to significantly different predictions of the tensile strength f_t of SFRC, although none of them may be intended to accurately predict the tensile behaviour of SFRC. For example, the tensile strength of mix H [MSF1 (35) + RTSF (10)] is predicted to be 3.41 MPa based on the RILEM approach, whist the strength is 2.05 MPa according to Model Code 2010. Since several studies [4,67] have reported overestimates of flexural behaviour of SFRC using the RILEM approach, it is proposed that for design purposes the same tensile strength as plain concrete is assumed for hybrid SFRC containing RTSF at a low total fibre dosage.

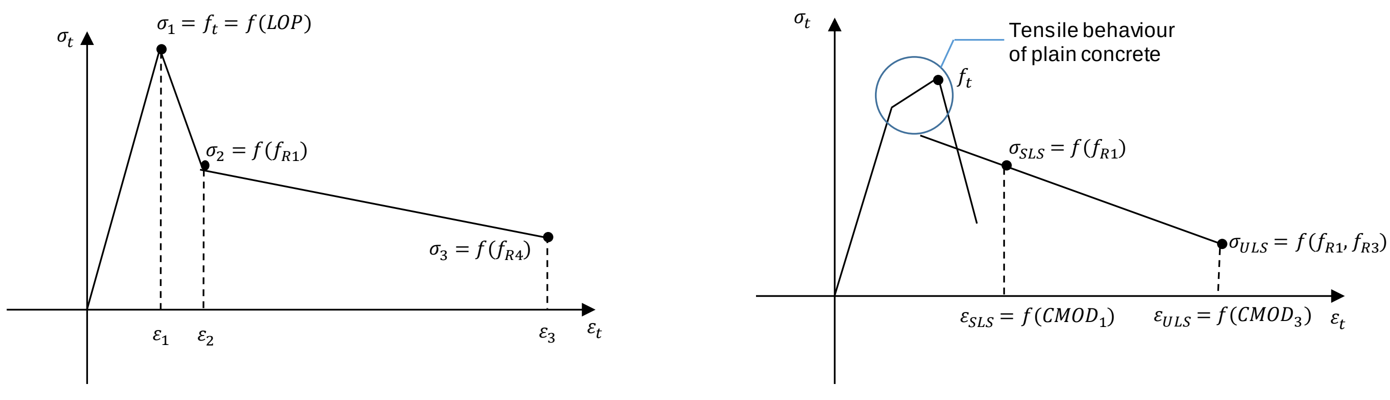

(a) (b)

Figure 22: Uniaxial tensile stress-strain diagrams for SFRC proposed by (a) RILEM TC 162-TDF (b) Model Code 2010

4.2 Residual flexural tensile strength and energy absorption capacity

The f_{R1} and f_{R2}, f_{R3} and f_{R4} values for SFRC prisms obtained in this study are strongly correlated. This implies that just two independent fracture parameters, e.g. f_{R1} and f_{R4}, are sufficient to represent the post-cracking behaviour of SFRC at small (i.e. the SLS) and large cracks (i.e. the ULS), respectively. Likewise, for the round panel tests, E_5 and E_{40} seem to be sufficient to quantify the flexural toughness of SFRC.

In current design guidelines for SFRC applications, two representative values of f_R out of four, are usually used: f_{R1}, along with f_{R3} or f_{R4}. For the design of SFRC ground-supported slabs at the Ultimate Limit state (ULS), the Concrete Society TR 34 [45] suggests that f_{R1} refers to the axial tensile strength at the crack tip, while the strength at the bottom crack opening is proportional to f_{R4} (Figure 23). For the determination of uniaxial tensile stress-strain diagrams of SFRC (see Figure 22), only f_{R1} and f_{R4} are used by RILEM TC 162-TDF [40], whilst only f_{R1} and f_{R3} are employed in Model Code 2010 [30].

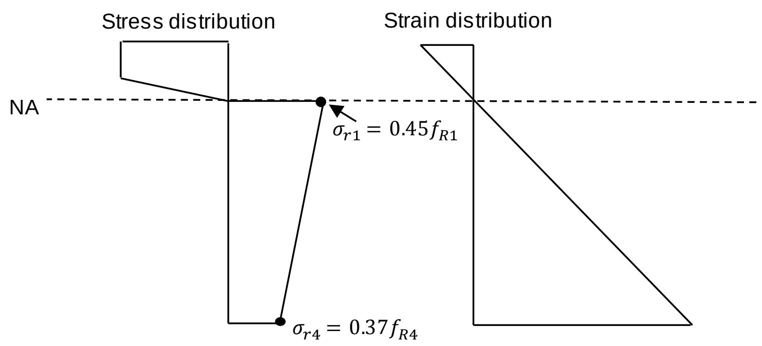

Figure 23: Stress block of a FRC floor section at the ULS (adopted by the Concrete Society TR 34)

4.3 Ground-supported slab thickness analysis

This section aims to quantify the effect of fibre type and dosage on the design of slab thickness, using the experimental results of the SFRC prisms examined in this study. As an example, a critical case for ground-supported slabs under flexure is considered, with two adjacent point loads (e.g. induced by back-to-back racking legs) applied near an edge of the slab. The design assumptions include a maximum leg load of 78 kN, a typical contact area of 100 mm×100 mm per leg, spacing between two racking legs of 300 mm, and radius of relative stiffness (the stiffness of concrete slab relative to that of sub-grade material) of 650 mm. The design flexural tensile strength of all SFRC mixes, is taken as 2 MPa, which is proposed to be the same as the design flexural tensile strength of plain concrete, according to the Concrete Society TR 34 [45].

Following the Concrete Society TR 34 design method for FRC ground-supported slabs, the relationship between required SFRC slab thickness (h) and the residual flexural tensile strengths f_{R1} and f_{R4} is given by Equation 10:

$$h \geq \sqrt{\frac{72655}{0.072 f_{R1} + 0.107 f_{R4} + 1.72}} \tag{10}$$

Figure 24 shows the relation between RTSF dosage for each of the SFRC mixes examined in this study and required slab thickness. As the total fibre dosage increased from 30 kg/m^3 to 45 (and 35) kg/m^3, the required slab thicknesses decreased, as expected. However, the required slab thicknesses did not vary considerably at the same total fibre dosage. Hybrid mixes B and H, both with 10 kg/m^3 of RTSF, exhibited the smallest slab thickness requirements.

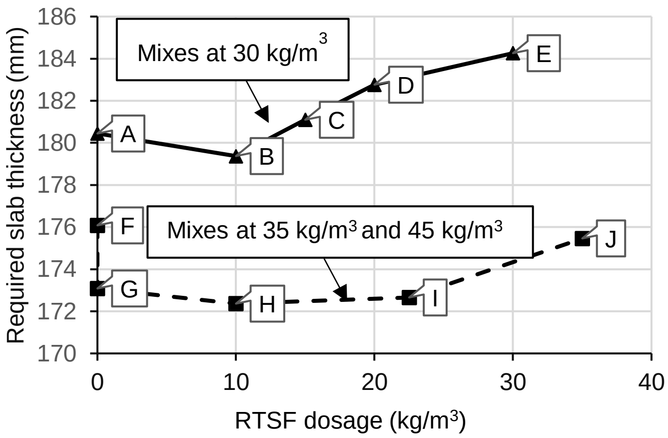

Figure 24: Relationship between RTSF dosage and required SFRC slab thickness for the examined SFRC mixes

The results demonstrate that hybrid mixes with RTSF can be competitive substitutes to MSF-only solutions for industrial concrete flooring applications. Such mixes could enable designs with less volume of concrete required, as well as up to 35 kg/m^3 MSF replacement with lower embodied energy fibres (i.e. RTSF).

5 CONCLUSIONS

The mechanical properties of 10 SFRC mixes using MSF and RTSF hybrids have been investigated by means of compressive cube, 3-point notched prism and round panel tests. The main research findings are:

- MSF and RTSF hybrids do not significantly affect f_{cu} and E_{fm}.

- RTSF are more effective in controlling microcracks. As cracks open, the flexural behaviour of SFRC depends increasingly more on fibre-matrix interaction, fibre orientation and distribution.

- Owing to the nonhomogeneous fibre distribution of SFRC, the variability of the fracture parameters obtained from prism tests was up to 35%, and up to 20% for round panels. The MSF and RTSF hybridisation has little effect on the scatter of the fracture parameters.

- Strong correlations exist between f_{R1} and f_{R2}, f_{R3} and f_{R4} (for prisms), as well as E_5 and E_{10}, E_{20} and E_{40} (for round panels). Correlations in the flexural behaviour of the SFRC prisms and round panels are reported. Proposed equations could be used by engineers to convert fracture parameters from one test to the other, but a wide testing database is still required.

- Hybrid mixes containing 10 kg/m^3 of RTSF at the total fibre dosage of 30 and 45 kg/m^3 offer significant synergetic effect. However, as the RTSF content increases, the performance drops below that of MSF-only mixes.

ACKNOWLEDGEMENTS

This research was funded by the EC collaborative FP7-ENV-2013-two-stage project "ANAGENNISI— Innovative Reuse of All Tyre Components in Concrete" under the grant agreement n° 603722 (www.anagennisi.org). The first author's PhD studies are sponsored by The China Scholarship Council (CSC number: 201508060086). The authors also thank Twincon Ltd for material supply and in-kind contributions.

REFERENCES

[1] ETRA, Introduction to tyre recycling: 2013, The European Tyre Recycling Association, Brussels, Belgium, 2013.

[2] WBCSD, End-of-life tires: a framework for effective management systems, http://www.wbcsd.org/DocRoot/lBTHZFGcpBK5OxTDXlpS/EndOfLifeTires_171208.pdf. 2010, (accessed 17. 07 .21).

[3] K. Pilakoutas, K. Neocleous, H. Tlemat, Reuse of tyre steel fibres as concrete reinforcement, Eng. Sustain. 157 (2004) 131–138.

[4] H. Tlemat, K. Pilakoutas, K. Neocleous, Stress-strain characteristic of SFRC using recycled fibres, Mater. Struct. 39 (2006) 365–377. doi:10.1617/s11527-005-9009-4.

[5] H. Tlemat, K. Pilakoutas, K. Neocleous, Modelling of SFRC using inverse finite element analysis, Mater. Struct. 39 (2006) 221–233. doi:10.1617/s11527-005-9010-y.

[6] K. Neocleous, H. Tlemat, K. Pilakoutas, Design issues for concrete reinforced with steel fibers, including fibers recovered from used tires, J. Mater. Civ. Eng. 18 (2006) 677–685. doi:10.1061/(ASCE)0899-1561(2006)18:5(677).

[7] A.G. Graeff, K. Pilakoutas, K. Neocleous, M.V.N.N. Peres, Fatigue resistance and cracking mechanism of concrete pavements reinforced with recycled steel fibres recovered from post-consumer tyres, Eng. Struct. 45 (2012) 385–395. doi:10.1016/j.engstruct.2012.06.030.

[8] N. Jafarifar, K. Pilakoutas, T. Bennett, Moisture transport and drying shrinkage properties of steel-fibre-reinforced-concrete, Constr. Build. Mater. 73 (2014) 41–50. doi:10.1016/j.conbuildmat.2014.09.039.

[9] K.H. Younis, K. Pilakoutas, Strength prediction model and methods for improving recycled aggregate concrete, Constr. Build. Mater. 49 (2013) 688–701. doi:10.1016/j.conbuildmat.2013.09.003.

[10] K.H. Younis, K. Pilakoutas, Assessment of post-restrained shrinkage mechanical properties of concrete, ACI Mater. J. 113 (2016) 267–276. doi:10.14359/51688699.

[11] H. Tlemat, Steel fibres from waste tyres to concrete, testing, modelling and design, The University of Sheffield, Sheffield, UK, 2004.

[12] A.G. Graeff, Long-term performance of recycled steel fibre reinforced concrete for pavement applications, The University of Sheffield, UK, 2011.

[13] K. Neocleous, H. Angelakopoulos, K. Pilakoutas, M. Guadagnini, Fibre-reinforced roller-compacted concrete transport pavements, in: Proceedings of the institution of civil engineers - transport, 2011: pp. 97–109. doi:10.1680/tran.9.00043.

[14] N. Jafarifar, Shrinkage behaviour of steel fibre reinfoced concrete pavements, The University of Sheffield, Sheffield, UK, 2012.

[15] H. Angelakopoulos, Reused post-consumer tyre steel fibres in roller compacted concrete, The University of Sheffield, Sheffield, UK, 2016.

[16] UFSD, Thin wire reinforcement for concrete. British Patent Application No 0130852.7 and 0511012.7, filed by The University of Sheffield on 24/12/01 and published on 9/11/2005, Sheffield, UK, 2001.

[17] H. Angelakopoulos, P Waldron, Tyre wire in Concrete Leading to Environmental sustainability. CIP Eco-innovation project, Twincletoes project - Layman’s report, Twincon Ltd, Sheffield, UK, 2015.

[18] K. Neocleous, S.G. Maxineasa, L. Dumitrescu, K. Themistocleous, N. Taranu and D. Hadjimitsis, D1.6

Preliminary LCA. Anagennisi Project, Anagennisi: innovative use of all tyre components in concrete, 2014.

[19] ACI 544.8R-16, Report on indirect method to obtain stress-strain response of fiber-reinforced concrete (FRC). American Concrete Institute, Michigan, US, 2016.

[20] E.S. Bernard, Influence of toughness on the apparent cracking load of fiber-reinforced concrete slabs, J. Struct. Eng. 132 (2006) 1976–1983. doi:10.1061/(ASCE)0733-9445(2006)132:12(1976).

[21] M. Colombo, M. di Prisco, L. Mazzoleni, Sprayed tunnel linings: a comparison between several reinforcement solutions, Mater. Struct. 42 (2009) 1295–1311. doi:10.1617/s11527-009-9528-5.

[22] V.S. Gopalaratnam, R. Gettu, On the characterization of flexural toughness in fiber reinforced concretes, Cem. Concr. Compos. 17 (1995) 239–254. doi:10.1016/0958-9465(95)99506-O.

[23] N. Banthia, M. Sappakittipakorn, Toughness enhancement in steel fiber reinforced concrete through fiber hybridization, Cem. Concr. Res. 37 (2007) 1366–1372. doi:10.1016/j.cemconres.2007.05.005.

[24] N. Banthia, J. Sheng, Fracture toughness of micro-fiber reinforced cement composites, Cem. Concr. Compos. 18 (1996) 251–269. doi:10.1016/0958-9465(95)00030-5.

[25] P. Rashiddadash, A.A. Ramezanianpour, M. Mahdikhani, Experimental investigation on flexural toughness of hybrid fiber reinforced concrete (HFRC) containing metakaolin and pumice, Constr. Build. Mater. 51 (2014) 313–320. doi:10.1016/j.conbuildmat.2013.10.087.

[26] N. Banthia, S.M. Soleimani, Flexural response of hybrid fiber-reinforced cementitious composites, ACI Mater. J. 102 (2005) 382–389.

[27] J.S. Lawler, T. Wilhelm, D. Zampini, S.P. Shah, Fracture processes of hybrid fiber-reinforced mortar, Mater. Struct. 36 (2003) 197–208. doi:10.1007/BF02479558.

[28] G. Tiberti, F. Minelli, G. Plizzari, Reinforcement optimization of fiber reinforced concrete linings for conventional tunnels, Compos. Part B. 58 (2014) 199–207. doi:10.1016/j.compositesb.2013.10.012.

[29] Y. Mohammadi, S.P. Singh, S.K. Kaushik, Properties of steel fibrous concrete containing mixed fibres in fresh and hardened state, Constr. Build. Mater. 22 (2008) 956–965. doi:10.1016/j.conbuildmat.2006.12.004.

[30] F.I. du Béton, Fib Model Code for Concrete Structures 2010, Wilhelm Ernst & Sohn, Berlin, Germany,2013.

[31] N. Banthia, N. Nandakumar, Crack growth resistance of hybrid fiber reinforced cement composites, Cem. Concr. Compos. 25 (2003) 3–9.

[32] L.G. Sorelli, A. Meda, G.A. Plizzari, Bending and uniaxial tensile tests on concrete reinforced with hybrid Steel Fibers, J. Mater. Civ. Eng. 17 (2005) 519–527. doi:10.1061/(ASCE)0899-1561(2005)17:5(519).

[33] E. Martinelli, A. Caggiano, H. Xargay, An experimental study on the post-cracking behaviour of Hybrid Industrial/Recycled Steel Fibre-Reinforced Concrete, Constr. Build. Mater. 94 (2015) 290–298. doi:10.1016/j.conbuildmat.2015.07.007.

[34] C.X. Qian, P. Stroeven, Development of hybrid polypropylene-steel fibre-reinforced concrete, Cem. Concr. Res. 30 (2000) 63–69. doi:10.1016/S0008-8846(99)00202-1.

[35] D. Bjegovic, A. Baricevic, S. Lakusic, D. Damjanovic, I. Duvnjak, Positive interaction of industrial and recycled steel fibres in fibre reinforced concrete, J. Civ. Eng. Manag. 19 (2013) S50–S60. doi:10.3846/13923730.2013.802710.

[36] K.H. Younis, K. Pilakoutas, M. Guadagnini, H. Angelakopoulos, Feasibility of Using Recycled Steel Fibres To Enhance the Behaviour of Recycled Aggregate Concrete, FRC 2014 Jt. ACI-Fib Int. Work. - Fibre Reinf. Concr.

from Des. to Struct. Appl. (2014) 598–608.

[37] A. Baricevic, D. Bjegovic, M. Skazlic, Hybrid fiber-reinforced concrete with unsorted recycled-tire steel Fibers, J. Mater. Civ. Eng. 29 (2017) 6017005. doi:10.1061/(ASCE)MT.1943-5533.0001906.

[38] Anagennisi Project, Anagennisi: innovative use of all tyre components in concrete. http://anagennisi.org/wordpress/, 2014 (accessed 2017.07.20).

[39] ACI 544.1R-96 (Reapproved 2002), State-of-the-art report on fiber reinforced concrete. American Concrete Institute, Michigan, US, 2002.

[40] Rilem Tc 162-Tdf, σ-ε-Design method, Mater. Struct. 36 (2003) 560–567. doi:10.1007/BF02480834.

[41] BS EN 14651:2005, Test method for metallic fibre concrete - Measuring the flexural tensile strength (limit of proportionality (LOP), residual). British Standards Institution, London, UK, 2005.

[42] BS EN 14488-3:2006, Testing sprayed concrete - Part 3: Flexural strengths (first peak, ultimate and residual) of fibre reinforced beam specimens. British Standards Institution, London, UK, 2006.

[43] BS EN 14488-5:2006, Testing sprayed concrete - Part 5: Determination of energy absorption capacity of fibre reinforced slab specimens, British Standards Institution, London, UK, 2006.

[44] BS EN 12390-5:2009, Testing hardened concrete - Part 5: Flexural strength of test specimens. British Standards Institution, London, UK, 2009.

[45] Technical report 34, Concrete industrial ground floors: a guide to their design and construction, The Concrete Society, Surrey, UK, 2013.

[46] ASTM C1018-97, Standard test method for flexural toughness and first-crack strength of riber-reinforced concrete (using beam with third-point loading), ASTM International, Pennsylvania, US, 1997.

[47] ASTM C1609/C1609M-05, Standard test method for flexural performance of fiber-reinforced concrete (using beam with third-point loading), ASTM International, Pennsylvania, US, 2005.

[48] ASTM C1550-05, Standard test method for flexural toughness of fiber reinforced concrete (using centrally loaded round panel), ASTM International, Pennsylvania, US, 2005.

[49] JSCE-SF4, Standard for flexural strength and flexural toughness, method of tests for steel fiber reinforced concrete, Concrete library of JSCE, Japan Concrete Institute (JCI), Japan,1984.

[50] B. Mobasher, Mechanics of fiber and textile reinforced cement, CRC Press, Florida, US, 2012.

[51] S. Oikonomou-mpegetis, Behaviour and design of steel fibre reinforced concrete slabs, Imperial College London, London, UK, 2012.

[52] F. Minelli, G.A. Plizzari, Fiber reinforced concrete characterization through round panel test - Part I: experimental study, in: Proceedings of the 7th international conference on fracture mechanics of concrete and concrete structures (FRAMCOS), 2010: pp. 1451–1460.

[53] BS EN 14889-1:2006, Fibres for concrete-Part 1: Steel fibres-definitions, specifications and conformity. British Standards Institution, London, UK, 2006.

[54] Z. Zamanzadeh, L. Lourenço, J. Barros, Recycled steel fibre reinforced concrete failing in bending and in shear, Constr. Build. Mater. 85 (2015) 195–207. doi:10.1016/j.conbuildmat.2015.03.070.

[55] A. Caratelli, A. Meda, Z. Rinaldi, Design according to MC2010 of a fibre-reinforced concrete tunnel in Monte Lirio, Panama, Struct. Concr. 13 (2012) 166–173. doi:10.1002/suco.201100034.

[56] G. Groli, A.P. Caldentey, A.G. Soto, Cracking performance of SCC reinforced with recycled fibres - an experimental study, Struct. Concr. 15 (2014) 136–153. doi:10.1002/suco.201300008.

[57] G. Groli, Crack width control in RC elements with recycled steel fibres and applications to integral structures: theoretical and experimental study, Polytechnical University of Madrid, Madrid, Spain, 2014.

[58] Q. Gu, H. Xu, S. Mindess, An improved test method and numerical analysis for crack opening resistance of FRC round determinate panels, Wuhan Univ. J. Nat. Sci. 14 (2009) 47–52. doi:10.1007/s11859-009-0111-2.

[59] E.S. Bernard, Correlations in the behaviour of fibre reinforced shotcrete beam and panel specimens, Mater. Struct. 35 (2002) 156–164. doi:10.1007/BF02533584.

[60] B.W. Xu, H.S. Shi, Correlations among mechanical properties of steel fiber reinforced concrete, Constr. Build. Mater. 23 (2009) 3468–3474. doi:10.1016/j.conbuildmat.2009.08.017.

[61] G. Centonze, M. Leone, M.A. Aiello, Steel fibers from waste tires as reinforcement in concrete: A mechanical characterization, Constr. Build. Mater. 36 (2012) 46–57. doi:10.1016/j.conbuildmat.2012.04.088.

[62] Ş. Yazıcı, G. İnan, V. Tabak, Effect of aspect ratio and volume fraction of steel fiber on the mechanical properties of SFRC, Constr. Build. Mater. 21 (2007) 1250–1253. doi:10.1016/j.conbuildmat.2006.05.025.

[63] M.A. Aiello, F. Leuzzi, G. Centonze, A. Maffezzoli, Use of steel fibres recovered from waste tyres as reinforcement in concrete: Pull-out behaviour, compressive and flexural strength, Waste Manag. 29 (2009) 1960–1970. doi:10.1016/j.wasman.2008.12.002.

[64] ACI 544.2R-89 (Reapproved 1999), Measurement of properties of fiber reinforced concrete. American Concrete Institute, Michigan, US, 1999.

[65] BS EN 12390-3:2009, Testing hardened concrete - Part 3: Compressive strength of test specimens. British Standards Institution, London, UK, 2009.

[66] M.N. Soutsos, T.T. Le, A.P. Lampropoulos, Flexural performance of fibre reinforced concrete made with steel and synthetic fibres, Constr. Build. Mater. 36 (2012) 704–710. doi:10.1016/j.conbuildmat.2012.06.042.

[67] J. a. O. Barros, V.M.C.F. Cunha, A.F. Ribeiro, J.A.B. Antunes, Post-cracking behaviour of steel fibre reinforced concrete, Mater. Struct. 38 (2004) 47–56. doi:10.1617/14058.

[68] R.D. Neves, J.C.O. Fernandes de Almeida, Compressive behaviour of steel fibre reinforced concrete, Struct. Concr. 6 (2005) 1–8. doi:10.1680/stco.6.1.1.62458.

[69] C.G. Papakonstantinou, M.J. Tobolski, Use of waste tire steel beads in Portland cement concrete, Cem. Concr. Res. 36 (2006) 1686–1691. doi:10.1016/j.cemconres.2006.05.015.

[70] B.I.G. Barr, M.K. Lee, E.J. de Place Hansen, D. Dupont, E. Erdem, S. Schaerlaekens, B. Schnütgen, H. Stang, L. Vandewalle, Round-robin analysis of the RILEM TC 162-TDF beam-bending test: Part 1-Test method evaluation, Mater. Struct. 36 (2003) 609–620. doi:10.1007/BF02483281.